Random dynamical response of Vulcain 1 engine during the transonic phase

*S. Frikha, A. Omrani, M. A. Hamdi**
**ESI Group, 99 rue des Solets - Silic 112 - 94513 Rungis – France*
*H. Lambare, L. Appolloni, D. Tchoukien, M. Illig ***
***CNES Evry Direction des Lanceurs*
Rond-point de l'Espace - Courcouronnes - 91023 Evry - France

Abstract
The paper presents an innovative approach to compute the random response of Vulcain engine submitted to aerodynamic loading at the transonic phase of the rocket launch.
Wall pressures are measured in a flow tunnel using a scaled prototype for a set of flow velocities and incidence angles. Pressure signals are processed into cross-spectral density matrices and extrapolated to real scale using similitude parameters. A dedicated module developed in RAYON® software allows the computation of modal coordinates of the aerodynamic pressure and the random response of the engine. Results obtained for Vulcain 1 has been successfully compared to reference results and in-flight measurements.

1. Introduction

The methodology described in this paper is an integral part of Cnes MINOS Program launched by Cnes in 2005. It aims to develop an integrated system of simulation tools allowing Cnes to carry out its role as a major actor in the domain of launchers system studies.
Simulation shall allow Cnes to carry out different studies on the several subjects under its responsibility. Activities range from preparation of future development programs for transportation systems, to exploitation of systems actually in production phase. It may address both tools at Cnes and research partners (Onera, DLR, and other research institutes), as well as a few tools coming from industry.
The objective of the MINOS Program is to develop necessary competences to be able to simulate any launcher system according to Cnes Launchers Directorate strategy, by the end of 2009. A first step is foreseen in 2007, at the same time of undergoing pre-development studies.
In the end, Cnes shall be capable to perform any cross-check study independently by industrial partners.
Several domains are addressed by the simulation program, ranging from technical tools to cost and programmatic aspects. MINOS is mainly dedicated to the technical fields.
Since many tools used for simulation are based on physical or theoretical models of an object or a system, there is a need for validating those models and quantifying their uncertainties, to be based on experimental approaches. For this reason, MINOS program is strictly connected with the R&T program of the Launcher Directorate, as well as with the ongoing development programs.

To respond to the expectations, several links are set-up with other existing environment, it is the case for example of the direct connexion between MINOS and the informatics and documentation network of Cnes, as well as the link to test databases coming from industry.

In this frame and in particular in the field of liquid propulsion, Cnes has expressed the need of developing an innovative approach to compute the random response of an engine submitted to

aerodynamic loading during the transonic phase of the rocket launch. The Vulcain 1 engine has been chosen as a first study case. The development and application of the methodology to this engine is described in the paper.
Merging both the numerical approach with the experimental results has allowed validating a good part of the procedure. In this respect, wall pressures are measured in a flow tunnel using a scaled prototype for a set of flow velocities and incidence angles. Pressure signals are processed into cross-spectral density matrices and extrapolated to real scale using similitude parameters. A dedicated module developed in RAYON® software allows to compute modal coordinates of the aerodynamic pressure and to calculate the random response of the engine. Results obtained for Vulcain 1 has been successfully compared to reference results and in-flight measurements.

2. Aerodynamic Pressure Measurement

The afterbody flow around the launcher Ariane 5 is characterized by a large separation because of an abrupt change in the geometry of the main stage. This generates strong low-frequency wall-pressure fluctuations, the base region being submitted to dynamic loads, especially during the high dynamic pressure phase of flight at transonic speeds. This aerodynamic excitation can induce a response of the structural modes called buffeting. In order to predict the resulting unsteady aerodynamic loads, wind-tunnel tests have been performed, in DNW's High Speed Wind Tunnel in Amsterdam, with a 1:60 Ariane 5 mock-up, equipped with a high number of unsteady wall pressure sensors on the afterbody. Furthermore, unsteady wall pressure on parts of the engine has been measured during flight, allowing correction of the wind-tunnel measurements. The vibrations of the engine nozzle and dynamic loads endured by the engine actuators have been also measured during flight. By applying the corrected pressure field on dynamic numerical models, vibrations and loads can be calculated and then compared to flight measurements, which validate the correction of the pressure field. Time histories of the unsteady pressures were processed into autopowers and cross-spectral densities (PSD) form, through a fast Fourier transform (FFT). The obtained PSD matrices are directly scaled to non-dimensional conditions using the Strouhal number (St). This is assumed to be valid for model and full-scale vehicle as well. Ref [1] contains further details about experimental set-up and unsteady wall-pressure measurements. The scaling procedure is detailed in Ref [2].

3. Dynamical response to Random aerodynamic excitation

3.1 Governing equation with partially correlated excitation

The particularity of the current problem is that the excitation is random and spatially distributed and partially coherent. Considering a mass normalized modal basis $\left[\tilde{W}\right]$, the movement equation expressed in the modal domain is:

$$\left[\Omega^2 - jD - \omega^2 \mathrm{I}\right]\left[S_{\alpha\alpha}\right]\left[\Omega^2 - jD - \omega^2 \mathrm{I}\right]^T = \left[S_{FF}\right] \tag{1}$$

where $S_{\alpha\alpha}$ is the cross spectrum matrix modal coordinate of the dynamical response, $\left[S_{FF}\right]$ is a cross spectrum matrix representing the modal coordinate the excitation, denoted here by modal forces, Ω and D are diagonal matrices composed of modal angular frequency and modal damping, [I] is the identity matrix and $[]^T$ denote the transpose conjugate. Solving equation (1) leads to:

$$S_{\alpha\alpha} = \left[\Omega^2 - jD - \omega^2 \mathrm{I}\right]^{-T} \left[S_{FF}\right]\left[\Omega^2 - jD - \omega^2 \mathrm{I}\right] \tag{2}$$

The power spectral density of the acceleration of a particular degree of freedom is obtained by modal synthesis as follows:

$$\gamma_k \gamma_k^{\,*} = S_{\gamma\gamma}(k,k) = \omega^4 \left\{\tilde{W}_k^{\,T}\right\}\left[S_{\alpha\alpha}\right]\left\{\tilde{W}_k\right\} \tag{3}$$

where $S_{\gamma\gamma}(k,k)$ is the acceleration Auto-spectrum of the k[th] degrees of freedom, $\tilde{W}_k$ contain the corresponding modal displacements. The Auto-spectrum of the internal forces and of the internal stresses is also obtained using a similar equation where the modal displacement γ_k is replaced by the modal internal force and modal stresses:

$$T_k T_k^{\,*} = S_{TT}(k,k) = \left\{\tilde{T}_k^{\,T}\right\}\left[S_{\alpha\alpha}\right]\left\{\tilde{T}_k\right\} \tag{4}$$

where the modal internal force $\tilde{T}_k$ is calculated during the modal analysis and is equal to the internal force (or internal stresses) obtained when the structure is vibrating following a unit amplitude single mode.

3.2 Modal coordinate of a partially correlated excitation

In the case of deterministic excitation, the modal coordinate of a distributed excitation is given by the Equation (1):

$$\tilde{F}_i = \sum_{e=1,Ne} \iint_{S(e)} F(x)\tilde{W}_i(x)dS \tag{5}$$

where N_e is the number of shell elements, $\tilde{W}(x)$ is modal shape, $F(x)$ is the force distribution (Force by unit surface) and $\tilde{F}_i$ is the modal force of the i[th] mode. The integral $\iint_{S(e)} F(x)\tilde{W}_i(x)dS$ represents the contribution of element "*e*" to modal force $\tilde{F}_i$ and is calculated using element shape function and force density at Gauss points. In the case of random and partially correlation excitation, the force distribution is defined by the cross spectrum density:

$$F(x_k, x_l) = F(x_k)F(x_l)^* \tag{6}$$

where the star (*) denotes the conjugate. This leads to partially correlated modal forces. The cross spectrum density of a couple of modal forces (*i*, *j*) is calculated as follows:

$$S_{FF}(i,j) = \tilde{F}_i \tilde{F}_j^{\,*} = \sum_{k=1,Ne} \sum_{l=1,Ne} \iint_{S(e_k)} \iint_{S(e_l)} \tilde{W}_i(x_k)F(x_k)F^*(x_l)\tilde{W}_j^{\,*}(x_l)dS_k dS_l \tag{7}$$

Here also, the double integral $\iint_{S(e_k)} \iint_{S(e_l)} \tilde{W}_i(x_k)F(x_k)F^*(x_l)\tilde{W}_j^{\,*}(x_l)dS_k dS_l$ gives the contribution of elements e_k and e_l to the cross spectrum between modal coordinate $\tilde{F}_i$ and $\tilde{F}_j$. It is calculated using element shape functions and the cross spectrum matrix between two set of Gauss point G_k and G_l. Therefore, the discrete form of equation (7) is as follow:

$$\left[S_{\tilde{F}\tilde{F}}\right]=\left[\tilde{W}\right]\left[A\right]\left[S_{GG}\right]\left[A^T\right]\left[\tilde{W}^T\right] \tag{8}$$

where $\left[S_{\tilde{F}\tilde{F}}\right]$ is the cross spectrum matrix of generalized modal forces, $\left[\tilde{W}\right]$ is the displacement modal basis and $\left[A\right]$ is an finite element (FE) interpolation operator, $\left[S_{GG}\right]$ is the cross spectrum matrix between the distributed random forces at Gauss points.
Substituting $\left[S_{\tilde{F}\tilde{F}}\right]$ using Equation (2) leads to:

$$\left[S_{\alpha\alpha}\right]=\left[\tilde{Z}\right]^{-T}\left[\tilde{W}^T\right]\left[A^T\right]\left[S_{GG}\right]\left[A\right]\left[\tilde{W}\right]\left[\tilde{Z}\right] \tag{9}$$

where $\tilde{Z}(\omega)=\left[\Omega^2-jD-\omega^2\mathrm{I}\right]$ is the classical modal dynamical stiffness matrix of the system.

3.3 Interpolation of cross spectral matrix at element Gauss points

The cross spectral matrix $\left[S_{GG}\right]$ is obtained from the measured cross-spectrum matrix using a geometrical interpolation method. For a given point X, the associated spectral density function is interpolated using the nearest spectral data of a set of surrounding sensors. This set may contain 2, 3 or 4 microphones. A weighting coefficient is associated to each microphone. As an example, when 3 microphones are used for the interpolation, the weighting coefficient associated to microphone 1 is:

$$\lambda_1(G)=\frac{d_2d_3}{d_2d_3+d_1d_2+d_1d_3} \tag{10}$$

where d_i is the distance between X and microphone m_i.
The cross-spectrum between the aerodynamic pressures at two Gauss points G_k, G_l is given by:

$$p(G_k)p^*(G_l)=\sum_{i=1}^{M}\sum_{j=1}^{N}\lambda_i\beta_j\,p(m_i)p^*(m_j) \tag{11}$$

Where N and M represent the numbers of microphones used to interpolate the pressure at G_k, and G_l, $\lambda_{i=1,N}$ and $\beta_{j=1,M}$ are the corresponding weighting coefficient and $p(m_i)p^*(m_j)$ is the cross spectrum between the pressure at microphone m_i and microphone m_j which represent the (i,j) term of the measured cross spectrum matrix $[S_{pp}]$.
This leads to the following expression of $[S_{GG}]$:

$$\left[S_{GG}\right]=\left[B^T\right]\left[S_{pp}\right]\left[B\right] \tag{12}$$

where the [B] is the interpolation operator allowing the extrapolation of the measured aerodynamic pressure to all the Gauss point of the outer-shell mesh of the engine, that would be used to calculate the modal forces. Substituting $[S_{GG}]$ in Equation (2) leads to:

$$[S_{\alpha\alpha}] = [\tilde{Z}]^{-T}[\tilde{W}^T][A^T][B^T][S_{pp}][\mathbf{B}][A][\tilde{W}][\tilde{Z}] \qquad (13)$$

3.4 Intermediate excitation mesh:

Equation (9) shows that the modal forces cross spectrum matrix need to be defined for all Gauss points of the outer shell subjected to the aerodynamic excitation. This leads to huge amount of cross-spectrum data. In order to reduce this amount of data and save both CPU and memory cost, the modal forces coordinates cross-spectrum matrix are calculated using a coarsened outer-shell mesh that will be denoted here as excitation mesh.
The modal eigenvectors are mapped onto the excitation mesh as follows:

$$[\tilde{W}_r] = [R][\tilde{W}] \qquad (13)$$

where [R] is the projection operator. Substituting in Equation (12) leads to:

$$[S_{\alpha\alpha}] = [\tilde{Z}]^{-T}[\tilde{W}^T][R^T][A^T][B^T][S_{pp}][\mathbf{B}][A][R][\tilde{W}][\tilde{Z}] \qquad (14)$$

In practice, the FE displacement field and the measured interpolation operators [A] and [B] are directly calculated considering the coarsened mesh which leads to:

$$[S_{\alpha\alpha}] = [\tilde{Z}]^{-T}[\tilde{W}_r^{\,T}][A_r^{\,T}][B_r^{\,T}][S_{pp}][\mathbf{B}_r][A_r][\tilde{W}_r][\tilde{Z}] \qquad (15)$$

where $[A_r]$ and $[B_r]$ are the interpolation operators for decimated excitation mesh.

4. Application to Vulcain 1

The methodology developed has been implemented in the RAYON® solver, developed by ESI Group, tacking advantage from its existing functionalities. Indeed, RAYON® solver offer validated capabilities for solving random dynamical response with uncorrelated or partially correlated excitation. On another side, RAYON® solver and is widely used to solve multi-domain vibroacoustic problem where incompatible mesh are generally considered.
The specificity of the case presented here is that the excitation is defined by a set of measured pressure distributed over the outer-shell of the structure. The interpolation procedure described in the previous section has been specifically implemented to calculate the cross-spectrum matrix of the generalised forces and to predict the random dynamical response of the Vulcain engine.
The aerodynamic excitation is applied to the external shell of the nozzle and the Thermal Protection (TP) of the engine. The excitation mesh has been obtained by decimating the original outer-shell mesh of the Vulcain engine (nozzle and thermal protection) by a factor of 5. The calculation of mapped mode shapes on the reduced mesh has been performed by the algorithm implemented in RAYON® software. Figure 1 shows an example of the original and the mapped mode shape (four-lobes-nozzle mode). It shows that the deformation of the nozzle is accurately reproduced on the decimated mesh.

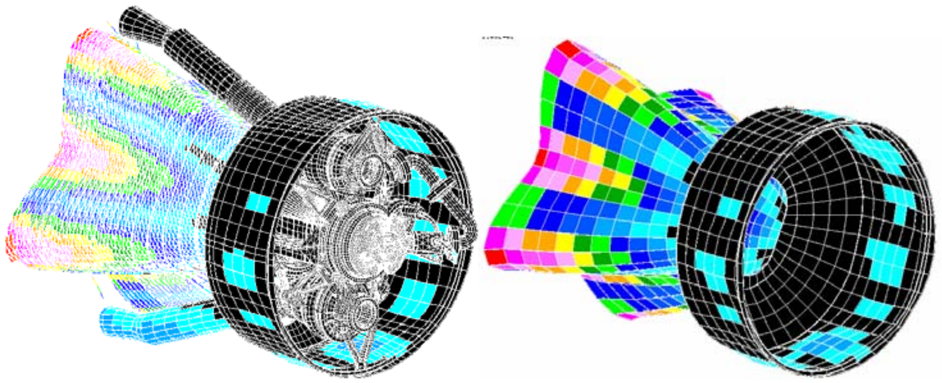

Figure 1: Mapped four-lobe nozzle mode shape on the excitation mesh. Original mode shape (left) – Projected mode shape (right mesh).

The wall pressure is measured on the engine nozzle and the thermal protection. Ninety flush-mounted pressure probes have been used to measure this excitation as shown in Figure 2. They are arranged in seven rings over witch five rings are on the nozzle and two rings are on the thermal protection.

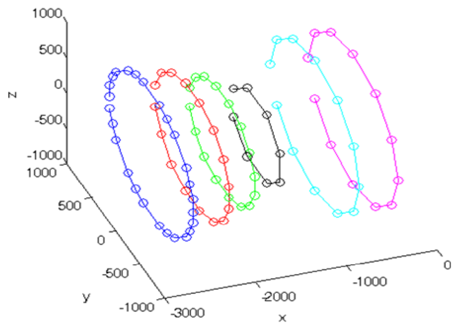

Figure 2: Location of Pressure sensors on the wall of the Engine Nozzle and the Thermal protection: 90 sensors are distributed over 6 rings. Four rings are on the nozzle (left side) and 2 rings are on the thermal protection (right side)

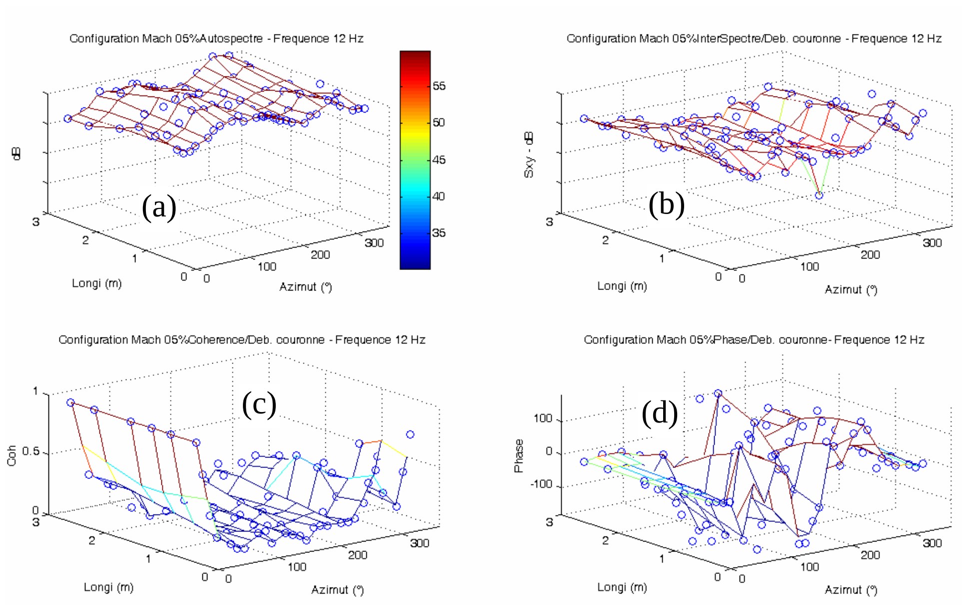

Figure 3: Azimuth Spectral density for each ring at 12 Hz. (a) Auto spectrum ; (b) Cross spectrum with respect to the first sensor of the ring – (c) coherence with respect to the first sensor of the ring – (d) phase of the cross spectrum with respect of the first sensor of the ring.

First, the spatial correlation has been investigated for considering each ring of sensor separately. Figure 3 shows the evolution of the spectral density, the cross spectrum and the pending coherence, at a particular frequency (12Hz). First graph (a) shows the pressure spectrum density along a ring. The pressure auto spectrum varies slightly over a ring. The cross spectrum and the coherence are plotted between each sensor and the first senor of the ring. One can notice that the spatial correlation (c) decreases rapidly to a value between 0.1 and 0.3. In the region where the coherence is low, the phase cross spectrum (d) is varying randomly.
The measurement has been performed for a set of configuration for various flow velocity and various incidence angles designed so as to rebuild the aerodynamic excitation during the transonic phase of the lift-off by rescaling and rearranging all the configurations.
For each configuration, the Power Spectral Density (PSD) of the acceleration at a set of nodes located on the nozzle and on the thermal protection has been computed. Two of these locations correspond to flight accelerometer. The rescaling and rearrangement of the obtained results for a set of configurations allow providing a prediction of the actual acceleration during the transonic phase. Figure 4 presents a comparison between the obtained results and reference results for Acc1 located on the bottom of the nozzle, during the transonic phase (starting at T0). A good matching is noticed over the whole period which demonstrates the validity of the presented approach.
Similar results are presented for the RMS in the 3-lobe frequency range in Figure 5. Here, the two accelerometers are presented. As for Acc1 , Acc2 is located on bottom of the nozzle shell and at 90° far from Acc1. So the results for ovalisation mode are almost the same. However, for 3-lobes modes, the results obtained for the two accelerometers are different as expected. Figure 5 show the good agreement with reference results for both accelerometers.

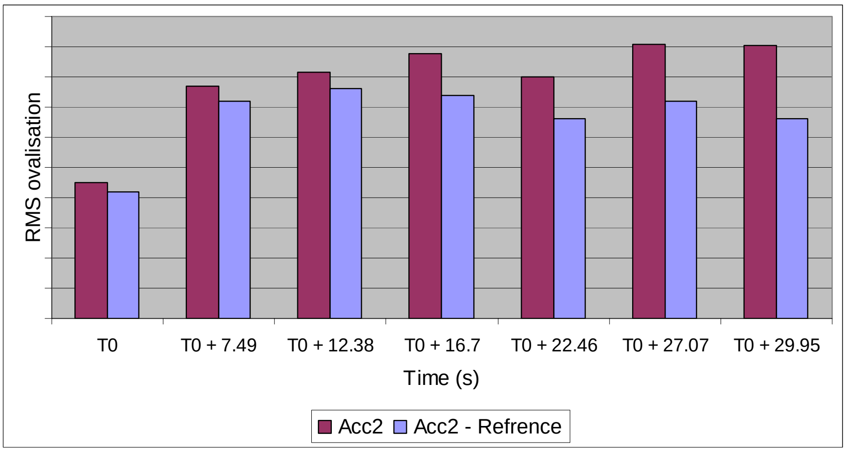

Figure 4: RMS of acceleration in the frequency range around the ovalization frequency of the nozzle shell.

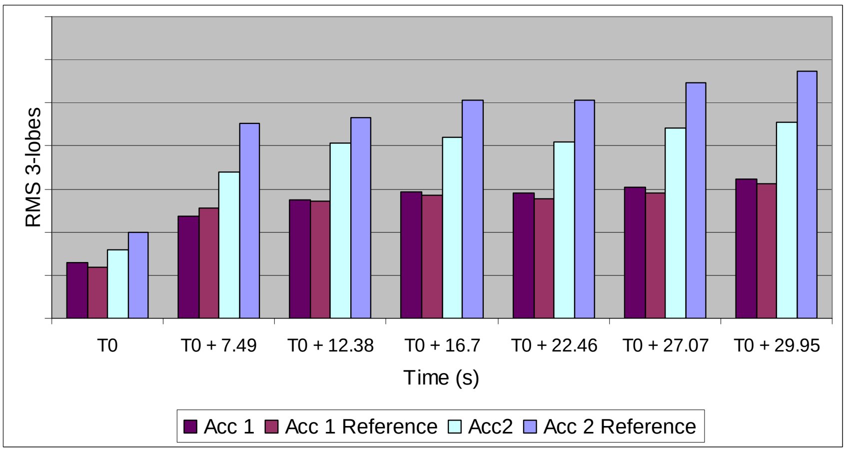

Figure 5: RMS of acceleration in the frequency range around the three-lobe frequency of the nozzle shell.

For the internal forces, the obtained results for each configuration have been processed to extract the global RMS over the whole frequency range. Therefore, the maximum RMS over all the configurations has been identified. In Figure 6, this maximum RMS is compared to the global effort calculated by CNES including aerodynamic and mechanical excitation as well. Results are presented for a set of 8 interfaces. Interface 1 to 6 (first subset) are expected to be mostly stressed in the transonic phase where aerodynamic force are dominant. Interface 7 and 8 (second subset) are expected to be mostly stressed in other phases where mechanical load are dominant. Figure 6 shows that the results obtained by RAYON® fit very well with the expected behaviour. Indeed, contribution of aerodynamic induced forces to global internal forces is between 30% and 80% for the first set of interface while their contribution remain lower than 20% for the second set.

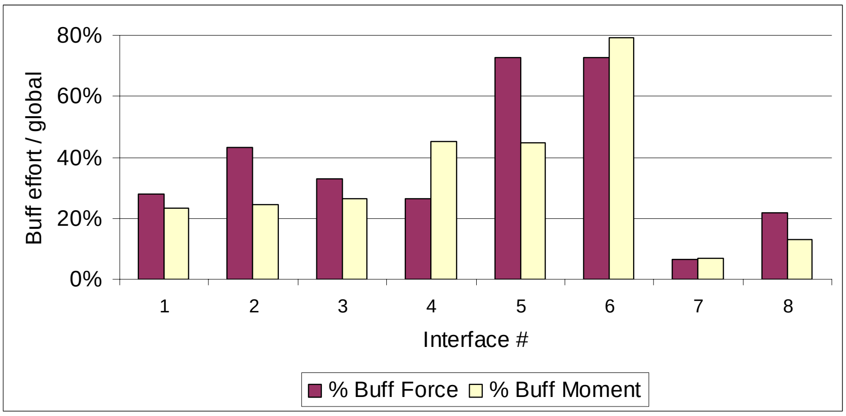

Figure 6: Contribution of aerodynamic excitation to the internal effort for 8 particular interfaces.

5. Conclusion

This paper presents a new methodology to calculate the dynamical response of a complex aerospace structure submitted to an aerodynamic loading. This excitation is characterized in the frequency-domain by a cross-spectrum matrix of the boundary layer pressure defined at a limited set of points. In the present case, these data are obtained using flow tunnel measurement on a scaled prototype. Similar Approach may be applied with pressure data obtained by Aerodynamic simulation (CFD). More specifically, the developed methodology, which is part of the CNES MINOS Program, allows an accurate simulation of the dynamical response of Ariane 5 Engine during the transonic phase where aerodynamic loading is significant. This methodology offers a very effective mixing of experimental approach used to characterize the aerodynamic loading and numerical simulation used to solve the random structural dynamic problem. The application to Vulcain 1 Engine, for which CNES has an extended prior knowledge, has been successfully performed. This proves the reliability of the whole approach.

References

[1] Geurts, E.G.M., “Steady and Unsteady Measurements on the Rear Section of Various Configuration of the Ariane 5 Launch Vehicle”, 6th International Symposium on Launcher Technologies, Germany, Nov. 2005.

[2] David, C., Radulovic, S.; Prediction of Buffet Loads on the Ariane 5 Afterbody, .6th International Symposium on Launcher Technologies, Munich, November 2005

[3] J-S. Bendat a,d A-G. Piersol. “Engineering Applications of correlations and spectral analysis”. Jhon Wiley & SON Inc. Second Edition 1993 ISBN 0-471-57055-9.

[4] P. H. Wirshing, and Al. “Random Vibrations – Theory and Practice”. Jhon Wiley & SON Inc. 1995. ISBN 0-471-58579-3

[5] RAYON Documentation and User Manual – ESI Group - 2006.

eucass

This page has been purposedly left blank